

Luminous hot accretion flows: the origin of X-ray emission of Seyfert galaxies and black-hole binaries

Feng Yuan^{1,2} and Andrzej A. Zdziarski³

¹*Harvard-Smithsonian Center for Astrophysics, 60 Garden Street, Cambridge, MA 02138, USA*

²*Department of Physics, Purdue University, West Lafayette, IN 47907, USA; fyuan@physics.purdue.edu*

³*Centrum Astronomiczne im. M. Kopernika, Bartycka 18, 00-716 Warszawa, Poland; aaz@camk.edu.pl*

Accepted 2004 July 28.

ABSTRACT

We investigate accretion disc models for the X-ray emission of Seyfert-1 galaxies and the hard state of black-hole binaries. We concentrate on two hot accretion disc models: advection-dominated accretion flow (ADAF) and recently found luminous hot accretion flow (LHAF). We solve for the global solution of both ADAF and LHAF to obtain the electron temperature, T_e , and Thompson optical depth, τ , at the radius where most of the radiation comes from. We adopt two kinds of electron energy equations. In one, only synchrotron and bremsstrahlung radiation and their Comptonization are considered. The other is parameterized by a constant Compton parameter to model the case in which thermal Comptonization of external soft photon is important. We compare the calculated T_e and τ with the observational values obtained by fitting the average spectra of Seyfert-1 galaxies and black-hole binaries using thermal Comptonization model. We find that the most favoured model is an LHAF with parameterized electron energy equation, with ADAFs predicting too high T_e . Also, the LHAF, but not ADAF, can explain large luminosities in excess of 10 per cent of the Eddington luminosity seen in the hard state of transient black-hole binaries.

Key words: accretion, accretion discs – black hole physics – galaxies: active – galaxies: nuclei – hydrodynamics – radiation mechanisms: thermal

1 INTRODUCTION

X-ray spectra of black-hole X-ray binaries in the hard state and Seyfert-1 galaxies usually consist of a power-law with a high-energy cutoff, Compton reflection, and Fe K α emission (e.g., Nandra & Pounds 1994; Zdziarski et al. 1995; Nandra et al. 1997). The cut-off power law is produced, most likely, by thermal Comptonization in a hot, mildly relativistic, plasma (see, e.g., Zdziarski & Gierliński 2004 for a review). Physical models for the hot plasma include a hot accretion disc, which we will discuss below, a magnetic-dominated corona (e.g., Galeev, Rosner & Vaiana 1979; Haardt & Maraschi 1993; Beloborodov 1999a), and an ion-illuminated accretion disc (Spruit & Haardt 2000; Deufel & Spruit 2000). Among them, the hot accretion disc model has the most clear dynamics and fewest free parameters, and we concentrate on that model in this paper.

Shapiro, Lightman & Eardley (1976, hereafter SLE) proposed the first hot accretion-disc solution. The available gravitational energy is converted in the process of viscous dissipation into the thermal energy of ions, which are much heavier than electrons. Since the only coupling between ions and electrons is Coulomb collisions which is rather weak,

and the radiation of electrons is much stronger than that of ions, the ion temperature, T_i , is much higher than that of electrons, T_e . The Thomson optical depth of the flow, τ , is low, so T_e can be as high as 10^9 K, high enough to produce X-ray photons. The SLE solution is thermally unstable (Pringle 1976). In addition, energy advection, which can be very important, is neglected in the energy equation of ions in SLE.

The second hot accretion-disc solution, advection-dominated accretion flow (ADAF; Ichimaru 1977; Rees et al. 1982; Narayan & Yi 1994, 1995; Abramowicz et al. 1995; see reviews by Narayan, Mahadevan & Quataert 1998; Kato, Fukue & Mineshige 1998), does include advection, which dominates the energy transfer for ions. The ion energy equation reads $q_{adv} = q_{vis} - q_{ie}$, with q_{adv} , q_{vis} and q_{ie} being the rates of energy advection, viscous heating and Coulomb cooling, respectively. In a typical ADAF, due to $\tau \ll 1$, $q_{ie} \ll q_{vis} \approx q_{adv}$, i.e., the viscous heating is balanced by advection cooling. We define a dimensionless accretion rate as

$$\dot{m} \equiv \frac{\dot{M}c^2}{L_E}, \quad (1)$$

where \dot{M} is the mass accretion rate, and L_E is the Eddington luminosity (note that in this definition we have not included the factor of 0.1 used by, e.g., Narayan & Yi 1995). With the increase of \dot{m} , since $q_{ie} \propto \dot{m}^2$ whereas $q_{vis} \propto \dot{m}$, q_{ie} increases faster than q_{vis} , Coulomb cooling becomes more and more important. When \dot{m} reaches a critical value, denoted as \dot{m}_1 here, we will have $q_{vis} \approx q_{ie}$, so advection fails to be the dominant cooling mechanism. We call \dot{m}_1 the critical rate of ADAF (Narayan, Mahadevan, & Quataert 1998). The existence of \dot{m}_1 and their low radiation efficiency make ADAFs rather dim. Therefore, this solution is very successful in explaining low luminosity/quiescent states of black-hole binaries and low-luminosity AGNs. However, it is not clear whether it applies to luminous X-ray sources such as Seyfert-1 galaxies and the luminous hard state of black-hole binaries.

Then, Yuan (2001, hereafter Paper I) found a new hot accretion solution above \dot{m}_1 , the so-called luminous hot accretion flow (LHAF). We emphasize that the equations describing LHAF are completely identical to those of ADAF, so LHAF is actually a natural extension of ADAF to accretion rates above \dot{m}_1 . In an LHAF, $\dot{m} > \dot{m}_1$, so we have $q_{vis} < q_{ie}$. The reason why hot solutions still exist above \dot{m}_1 is that the compression work, q_{com} , provides additional heating in addition to q_{vis} , so $q_{com} + q_{vis} > q_{ie}$ (see Paper I for details) if \dot{m} is not too large. Since $q_{adv} = q_{vis} - q_{ie} < 0$, advection plays a heating rather than a cooling role in LHAF. In other words, the entropy of the accretion flow in an LHAF is converted into radiation, similar to the cases of spherical accretion and cooling flow in galactic clusters¹.

A unified description of the three hot accretion disc models, namely the SLE solution, ADAF and LHAF, has been presented in Yuan (2003). Yuan (2003) has also shown that if thermal conduction is neglected, LHAF is thermally unstable under local perturbations. However, the timescale of the growth of the thermal perturbations is in general longer than the accretion timescale if \dot{m} is not too large, despite the relatively strong radiative cooling in LHAF, so the solution can survive. Furthermore, inclusion of thermal conduction generally has a very strong stabilizing effect.

From ADAF to LHAF, both the accretion rate and the radiation efficiency increase continuously (but the efficiency is still lower than in the standard thin disc), so LHAFs are significantly more luminous than ADAFs. Thus, LHAFs offer a promising solution to the problem of the nature of X-ray emission of luminous accreting black holes. Here, by comparing the predictions of the ADAF and LHAF solutions for the T_e , τ , and the bolometric flow luminosity, L , with results of fits to hard X-ray observations, we investigate

¹ We expect the existence of solutions which are ADAFs far from the black hole and become LHAFs at smaller radii when \dot{m} is not very large, because the radiative cooling rate, q_{rad} , is very low at large radii. Such solutions were not presented in Paper I. We find that they do exist, but only in a narrow range of \dot{m} . This narrowness is, in fact, due to the definition of LHAF as satisfying $q_{vis} < q_{ie}$. If, instead, we define LHAF solutions as those satisfying $q_{vis} < q_{rad}$, we would have found the corresponding ADAF-LHAF transition solutions in a wider range of \dot{m} . This is because at $R \gg 10^2 R_s$, $q_{ie} \gg q_{rad}$, where $R_s \equiv 2GM/c^2$. On the other hand, the two cases become identical at small radii, $R \lesssim 10^2 R_s$.

which of these two solutions is more appropriate to describe the nature of X-ray emission of luminous black hole sources.

X-ray emission of Seyfert galaxies and black-hole binaries in the hard state is most likely due to thermal Comptonization of soft photon by thermal hot electrons. For a given geometry, the thermal-Comptonization spectrum is determined by two parameters of the hot plasma, the electron temperature, T_e , and the Thompson optical depth, τ . Fits with this model, summarized in Section 2 below, provide observational constraints on T_e and τ , as well as on L . We then compare them with the values predicted by the ADAF and LHAF global solutions.

On the theoretical side, the exact cooling mechanism of electrons remains unknown. In particular, Comptonization of synchrotron radiation photons may be not the dominant process in luminous X-ray sources. Evidence supporting this point includes a correlation between the strength of Compton reflection and the X-ray spectral index (Zdziarski, Lubiński, & Smith 1999; Zdziarski et al. 2003) and theoretical arguments showing that this process is often not capable to provide the required flux of seed photons required (SLE; Zdziarski et al. 1998; Wardziński & Zdziarski 2000).

Sources of soft photons other than the synchrotron emission are, however, very likely to exist. The soft photons can come from a cold disc just outside of, or penetrating into, an inner hot accretion flow, if the truncation radius of the cold disc is not too large (Poutanen, Krolik & Ryde 1997; Zdziarski et al. 1999). Another possibility is that the accretion flow consists of two phases, with some cold clouds or clumps embedded in the hot accretion gas (Guilbert & Rees 1988; Celotti, Fabian & Rees 1992; Kuncic, Celloti & Rees 1997; Krolik 1998). In this case, the emission from the clumps can serve as the seed photons of Comptonization. There is also very strong observational evidence for cold medium extending close to the black hole in Seyferts and black-hole binaries from relativistic broadening of the reflection/reprocessing features (e.g., Nandra et al. 1997; Życki, Done & Smith 1998). In accord with those observations, the LHAF model predicts that when \dot{m} is very high, the hot flow can collapse and form an optically-thick disc in the innermost region (Paper I), which disc will also be a copious source of soft photons.

For those reasons, the determination of the electron energy equation can be very complicated. An approach to overcome this difficulty is to parameterize the energy equation of electrons using the Compton parameter,

$$y = 4\tau \frac{kT_e}{m_e c^2}, \quad (2)$$

where $\tau = \sigma_T n_e H$ corresponds to the disc scale height, H , σ_T is the Thomson cross section, $m_e c^2$ is the electron rest energy, and n_e is the electron density. A given value of y corresponds quite well to the X-ray photon index Γ (Ghisellini & Haardt 1994; Poutanen 1998; Beloborodov 1999b), which is observationally well constrained. Note that some other definitions of y also exist, modifying the above expression for the cases of large τ and relativistic T_e . In particular, Beloborodov (1999b) used the definition of $y = 4[kT_e/m_e c^2 + 4(kT_e/m_e c^2)^2](\tau + \tau^2)$, for which case he found

$$\Gamma \simeq \frac{9}{4} y^{-2/9} \quad (3)$$

in a spherical geometry.

Furthermore, y (or, equivalently, Γ) is often almost constant with varying flux for luminous black-hole sources (e.g., Cyg X-1, Gierliński et al. 1997; GX 339-4, Zdziarski et al. 1998, 2004; Wardziński et al. 2002; IC 4329A, Fiore et al. 1992), which tells us that the relative cooling rate is typically more stable than the X-ray flux from the source. Then, instead of considering the various sources of soft photons, we replace the electron energy equation by assuming that there is a local source of seed photons leading to a given parameter y , and solve for the disc equations. This is in fact the approach adopted by SLE (who assumed $y = 1$), and by Zdziarski (1998), who generalized the hot disc model of SLE by including energy advection in the ions energy equation and allowing y to be a free parameter.

We present the data we use in Section 2. In Section 3, we solve the radiation-hydrodynamic accretion equation parameterized by Compton parameter, y . For completeness, we also investigate the standard case, where only Comptonization of synchrotron and bremsstrahlung photons is taken into account. The results are presented in Section 4. We then discuss our results in Section 5 and present our conclusions in Section 6.

2 THERMAL COMPTONIZATION IN ACCRETING BLACK HOLES

Table 1 summarizes best-fit plasma parameters of thermal Comptonization models fitted to Seyferts and two black-hole binaries in the hard state. This model has been found to fit the observed spectra rather well. We see that the fitted parameters cover a remarkably narrow range of the electron temperature, $kT_e \simeq 50\text{--}100$ keV. A similarly narrow range is obtained for the Thomson optical depth; the corresponding range for spherical geometry is $\tau \simeq 2.5\text{--}1.5$. For clarity, the uncertainties are not given in Table 1; however, the best-fit values from a rather large number of fits all fall within the above range, which confirms the statistical significance of this result. The points for spherical geometry (and including results of fits of hybrid plasma) are shown in Fig. 1. Those points were mostly obtained with the highly accurate Comptonization model of Poutanen & Svensson (1996).

In the case of Seyferts, the data existing so far are mostly insufficient to constrain the parameters of the Comptonizing plasma, with the exception of the Seyfert brightest at ~ 100 keV, NGC 4151. To circumvent this problem, average spectra from some sets of observations were formed (Nandra & Pounds 1994; Zdziarski et al. 1995; Gondek et al. 1996; Zdziarski, Poutanen, & Johnson 2000, hereafter ZPJ). Among them, only ZPJ fit the resulting average spectra with thermal Comptonization, and thus we use their results here.

We note that ZPJ used as free parameters kT_e and y instead of τ . To be able to show the results in our Fig. 1, we have refitted the average spectrum of Seyfert 1s in the $kT_e\text{--}\tau$ space with the same assumptions as in ZPJ. Their data are from the OSSE detector aboard *Compton Gamma Ray Observatory*, which covers the energy range of above 50 keV only. Data below 50 keV provide then additional constraints. However, the data sets of ZPJ were found to be compatible with the range of the X-ray photon spectral index of $\Gamma \sim 1.5\text{--}2.3$, which corresponds quite well to the range observed in Seyferts (e.g., Nandra & Pounds 1994;

Table 1. Hot plasma parameters in accreting black holes.

Object	kT_e [keV]	τ^a	Geometry	Reference ^b
average Sy 1	69	1.6	sphere	ZPJ
average Sy 2	84	1.7	sphere	ZPJ
NGC 4151	73	1.5	sphere	7
	65	1.5	sphere	ZPJ
	62	2.0	hemisphere	3
Cyg X-1	100	2.0	hemisphere	2
	100	1.3	sphere	2
	59	1.9	sphere	1
	58	2.9	sphere ^c	4
GX 339-4	52	0.9	slab	6
	57	2.0	sphere	6
	46	2.5	sphere	5
	43	2.7	sphere	5
	58	1.9	sphere	5
	46	2.2	sphere	5
	76	1.5	sphere ^c	5

^a along the radius for sphere/hemisphere, and half-thickness for a slab.

^b 1: Frontera et al. (2001); 2: Gierliński et al. (1997); 3: Johnson et al. (1997); 4: McConnell et al. (2002); 5: Wardziński et al. (2002); 6: Zdziarski et al. (1998); 7: Zdziarski et al. (2002).

^c A hybrid (Maxwellian with a tail) electron distribution assumed.

Zdziarski et al. 1999, 2003). In the contour shown in Fig. 1, the end with the lowest τ and the highest kT_e corresponds to the softest spectra, with $\Gamma \sim 2.2\text{--}2.3$, whereas the opposite end corresponds to $\Gamma \sim 1.5$. Thus, the extent of this error contour actually corresponds to the range of the observed Γ . It is also remarkable that this error contour agrees relatively well with the best-fit parameters of a number of individual accreting black holes (for the same geometry).

3 THE EQUATIONS AND NUMERICAL APPROACH

We concentrate on the inner region of the accretion disc since most of the radiation comes from it. We adopt the potential of Paczyński & Wiita (1980) to mimic the geometry of the central Schwarzschild black hole. Steady axisymmetric and two-temperature assumptions to the accretion flow are adopted as usual. A randomly oriented magnetic field is assumed to exist in the accretion flow and the magnetic pressure is in equilibrium with the gas pressure. We further assume that the accretion rate is independent of radius and the viscous dissipation mainly heats ions. We will discuss the validity of these two assumptions in Section 5.

With these assumptions, we can write down the equations describing the dynamics of the hot accretion flow (ADAF & LHAF). These equations include the conservations of mass and momentum fluxes, and the energy equations of ions and electrons. For the case of the standard electron energy equation, these equations are the same as in Paper I. In particular, cooling due to Comptonization in

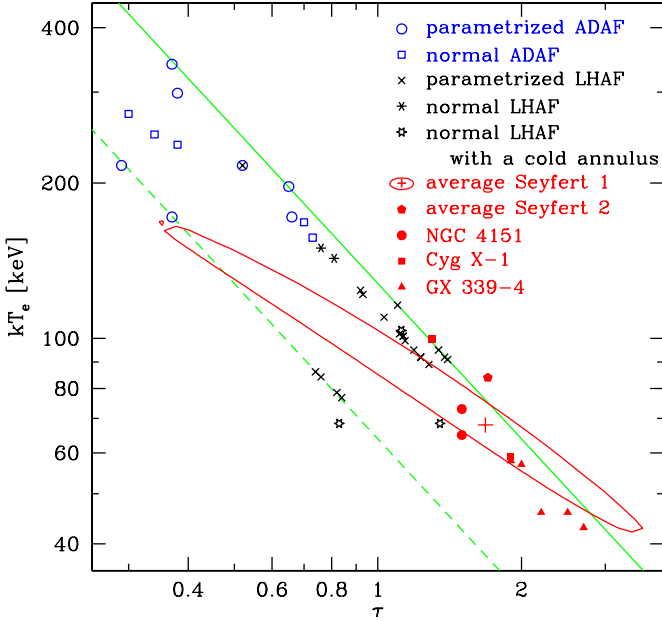


Figure 1. The observed parameters, electron temperature, kT_e and Thompson optical depth, τ , of a number of accreting black holes compared to results of two hot accretion models, ADAF and LHAF. The contour corresponds to the average Seyfert-1 spectrum of ZPJ. The model points are from Tables 2 and 3 but excluding the case of $\alpha = 0.01$. The solid and dashed lines correspond to $y = 1$ and 0.5 , respectively.

that case is treated using a local energy enhancement factor (Dermer, Liang, & Canfield 1991; Esin et al. 1996). On the other hand, Comptonization of external soft photons is taken into account by using the energy equation of electrons parametrized by the Compton parameter, analogously to Zdziarski (1998).

The numerical approach is also the same with in Paper I. The physical solutions should satisfy the sonic point condition, the zero-torque condition at the horizon, and an outer boundary condition (OBC). Since we are interested in the inner region of the disc, we set the radius of the outer boundary at $R_{\text{out}} = 10^2 R_s$. Our solution is self-consistent since we simultaneously solve the coupled radiation-hydrodynamical equations including the energy equations of both ions and electrons. This ensures that our obtained values of T_e and τ are exact enough to be compared with the observations.

The OBC is found to play an important role in determining some details of the ADAF, such as the value of T_e (Yuan 1999; Yuan et al. 2000). This is because the *differential* terms such as that describing the advection of energy play an important role in the equations, so the description of accretion is mathematically a boundary-value problem. Because the equations describing ADAFs and LHAFs are completely identical, we expect similar effect exists for LHAFs as well. We therefore should choose the OBC reasonably based on some physical considerations. For example, if the hot flow is formed by some processes from an outer cold disc, we should consider the transition process. An understanding of such process is still lacking. However, it was found that physical accretion solutions exist only for a range of T_e and T_i at the OBC (Yuan 1999). The actual range depends on the parameters of the flow. For example, when \dot{m} is high and

R_{out} is large, the range is small, hence the effect of OBC is not very important.

We set the T_e and T_i at the outer boundary at any values for which we can obtain a physical solution. There is no difference in this respect between the ADAF and the LHAF. Due to the finite range of the allowed OBC, such a solution is not unique. However, we confirm that for both ADAFs and LHAFs the allowed ranges are narrow, and thus the effect of the OBC does not affect our results. The main reason for this is that the mass accretion rates we consider are relatively high. Another reason, in the case of parameterized energy equation, is that the differential equation is replaced by an algebraic one.

We would like to emphasize that the narrowness of the range of the OBCs depends on the numerical method adopted. Two methods to obtain global solutions of accretion flows are generally used, namely the shooting and relaxation ones. When the (more accurate) shooting method is adopted, as in the present paper, the narrowness of the OBC is universal for the global solutions of any accretion models (e.g., ADAFs, Nakamura et al. 1997; slim disc, Abramowicz et al. 1988). It does not imply the solution cannot be realized in nature. When the OBC of a flow is out of this narrow range, it is likely that the flow can adjust itself to find the actually existing solution by some other physical processes, e.g., thermal conduction, or the solution can be weakly time-dependent on the viscous time scale.

4 RESULTS

4.1 Seyfert galaxies

4.1.1 The parameterized electron energy equation

We first calculate the critical mass accretion rate, \dot{m}_1 , of an ADAF parameterized by the Compton parameter y , assuming $M = 10^8 M_\odot$. The usual advection factor is defined as $f \equiv q_{\text{adv}}/q_{\text{vis}}$. The canonical ADAF has $f \approx 1$, an ADAF at the critical rate has $f \simeq 0$, while an LHAF has $f < 0$. Since f is a function of radius, we define the critical rate, \dot{m}_1 , as the maximum rate at which f for the corresponding solution is still > 0 at all radii, see the dashed curve in Fig. 2(b). With this definition, we find that for $R_{\text{out}} = 10^2 R_s$, \dot{m}_1 of ADAFs parameterized by y is 0.04, 0.4, 1, 2, 0.5 for $(\alpha, y) = (0.01, 1)$, $(0.05, 1)$, $(0.1, 1)$, $(0.3, 1)$, $(0.1, 0.5)$, respectively. Very approximately, $\dot{m}_1 \simeq y(\alpha/0.1)^{1.4}$ for $\alpha \lesssim 0.1$, similar to $\dot{m}_1 \sim 10y^{0.6}\alpha^{1.4}$ obtained by Zdziarski (1998).

In Paper I, we found that LHAF has two possible structures depending on the accretion rate. When $\dot{m}_1 \lesssim \dot{m} \lesssim \dot{m}_2$, the accretion flow remains hot throughout the disc. Here $\dot{m}_2 \sim 5\dot{m}_1$, and its exact value depends on the flow parameters and the OBC. When $\dot{m}_2 \lesssim \dot{m} \lesssim 10$, the Coulomb cooling of the ions becomes so efficient (due to the high density) within certain radius that the accretion flow collapses onto the equatorial plane and forms a cold, optically-thick, annulus. Similarly in the present case of the parameterized energy equation, there are also two types of LHAF, one remaining hot throughout the disc and the other collapsing and forming a cold optically-thick annulus within a certain radius. Note that we assume that the cooling of the hot plasma by the optically-thick emission of the cold annulus is included in our parameterized electron energy equation.

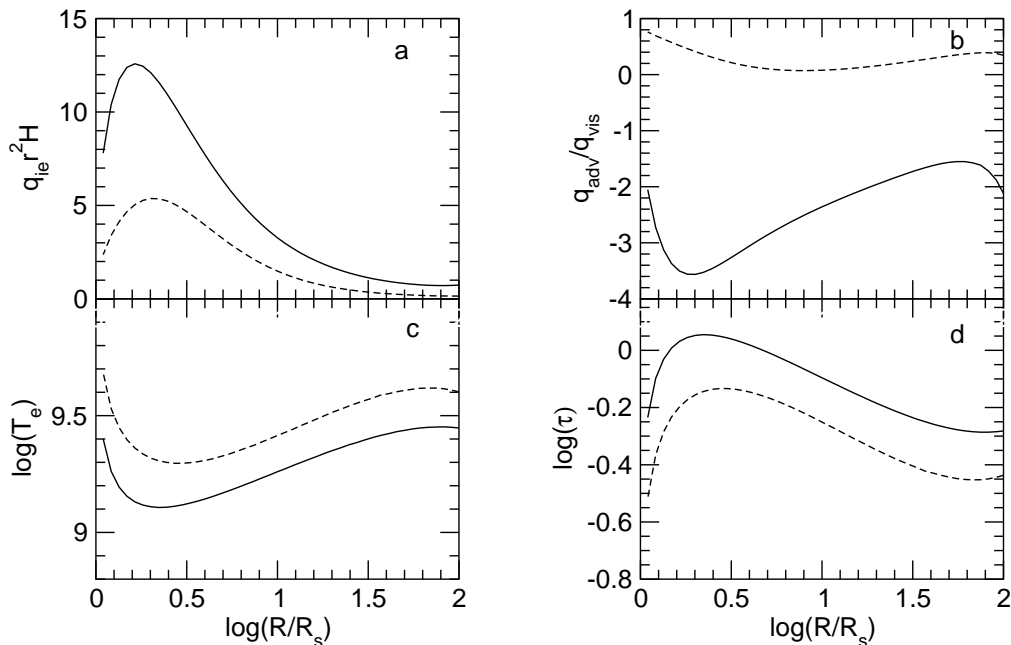


Figure 2. The radial variation of the radiation rate, $q_{ie}Hr^2$ (in dimensionless units with $M = G = c = 1$ and multiplied by a factor of 10^{17}), the advection factor, q_{adv}/q_{vis} , T_e and τ , for two hot disc solutions with the parameterized electron energy equation. The dashed curves correspond to an ADAF solution, with $\alpha = 0.3$, $y = 0.89$, $\dot{m} = 2$ ($\approx \dot{m}_1$), and the OBC at $T_i = 8 \times 10^9$ K, $T_e = 4 \times 10^9$ K. The solid curves correspond to an LHAF solution, with $\alpha = 0.3$, $y = 0.89$, $\dot{m} = 4$, and the OBC at $T_i = 9 \times 10^9$ K, $T_e = 2.8 \times 10^9$ K.

Fig. 2 shows two examples of the global solution, with the dashed curve denoting a critical ADAF and the solid curve an LHAF. The four panels show the radial profiles of T_e , $q_{ie}r^2H$, τ , and q_{adv}/q_{vis} . We see that the T_e and τ depend on radii. This presents us an issue of which values of T_e and τ are most representative for the emitted spectra, and can then be compared with results of fits to data with Comptonization in a uniform plasma. We see in Fig. 2(a) that the emission rate per logarithm of radius, proportional to $q_{ie}r^2H$, show rather strong maxima, both for the ADAF and the LHAF. We find it to be generally the case, both for the standard and the parameterized electron energy equation. Therefore, we compare the values of T_e and τ at this maximum with the observational data.

Since the maximum peak is generally sharp, a uniform slab appears to be an approximation to the flow geometry somewhat worse than that of a sphere. On the other hand, the actual flow geometry is still flattened, and the values of τ obtained in the spherical geometry should be somewhat decreased when compared to the hot-flow results. In the case of a uniform slab, the fitted τ of the half-thickness is lower by a factor of $\gtrsim 2$ from the radial τ fitted in the spherical geometry (e.g., ZPJ). We thus estimate that the values of τ obtained from fits in spherical geometry should be reduced by a factor of ~ 1.5 when compared with the τ of a hot flow calculated as above. Note that this correction also implies that the values of y used in the hot flow models should be correspondingly reduced to correspond to the data.

Our results, including the model luminosity, for the parameterized electron energy equation are given in Table 2, and the obtained values of kT_e and τ are also shown in Fig. 1. The luminosity is calculated assuming the electrons radiate away all the energy obtained from Coulomb collisions,

which is a good approximation at high accretion rates. The luminosity for solutions with a cold annulus is given only for the hot flow, i.e., not including that of the annulus. We consider $\alpha = 0.01, 0.1, 0.3$, and $y = 0.5, 0.89, 1$. The middle value of y corresponds to the best fit to the average Seyfert-1 spectrum by ZPJ (but without correcting for the difference between geometries of the flow geometry and of a sphere). The considered range of y roughly corresponds to the range of the 2–10 keV spectral index most common in Seyferts, $\Gamma \sim 1.7$ –2.1 (Nandra & Pounds 1994; Zdziarski et al. 1999).

Our goal is to check which accretion models yield T_e and τ in agreement with the observational data for luminous sources. For the ADAF, we only show solutions with $\dot{m} \sim \dot{m}_1$ since solutions with a lower \dot{m} would yield values of T_e clearly much higher than those observed.

For $\alpha = 0.1, 0.3$ and $y = 0.5, 0.89, 1$, we find that T_e for parameterized ADAFs is $\geq 10^{9.3}$ K, while it is $10^{8.9}$ K $\leq T_e \leq 10^{9.2}$ K for parameterized LHAFs. The agreement between the predictions of the LHAF solution and the observations is very good. We therefore conclude that these LHAF solutions (with additional cooling responsible for the observed values of y) are very likely to correspond to the actual accretion flows in Seyfert-1 galaxies.

We have also considered $\alpha = 0.01$. We find that in this case neither ADAF nor LHAF can be reconciled with the data because of the too high T_e predicted. This provides an interesting observational constraint on the viscous parameter, $\alpha \gtrsim 0.1$. If the viscous stress is caused by magnetic field via the magneto-rotational instability, the numerical simulation by Hawley, Gammie & Balbus (1996) imply $\alpha \gg 0.01$ (with $\alpha \sim 0.4$ for equipartition magnetic field), in agreement with our constraint.

In our calculations, we assume that the Compton pa-

Table 2. Model parameters of some parameterized hot disc solutions.

Number	Type ^a	α	y	\dot{m}	$\log(T_e [\text{K}])$	τ	$L/L_E [\%]$
1	ADAF	0.3	0.89	1($< \dot{m}_1$)	9.54	0.38	0.8
2	ADAF	0.3	0.89	2($\approx \dot{m}_1$)	9.3	0.66	3.6
3	LHAF	0.3	0.89	4	9.15	0.93	6.4
4	LHAF	0.3	0.89	4	9.01	1.28	10.2
5	LHAF	0.3	0.89	5	9.04	1.19	6.5
6	LHAF	0.3	0.89	5	9.03	1.23	5.0
7	LHAF	0.3	0.89	6	9.07	1.13	4.0
8	LHAF	0.3	0.89	6	9.06	1.14	3.5
9	LHAF ^b	0.3	0.89	5	9.074	1.11	2.5
10	LHAF ^b	0.3	0.89	6	9.069	1.13	3.2
11	ADAF	0.3	0.5	1($< \dot{m}_1$)	9.3	0.37	1.0
12	ADAF	0.3	0.5	1($< \dot{m}_1$)	9.4	0.29	1.0
13	LHAF	0.3	0.5	2($> \dot{m}_1$)	8.95	0.84	8.3
14	LHAF	0.3	0.5	4	8.96	0.82	3.0
15	LHAF	0.3	0.5	5	8.99	0.76	2.5
16	LHAF	0.3	0.5	8	9.0	0.74	3.2
17	ADAF	0.3	1.0	1($< \dot{m}_1$)	9.6	0.37	0.7
18	ADAF	0.3	1.0	2($\approx \dot{m}_1$)	9.36	0.65	3.5
19	LHAF	0.3	1.0	4	9.03	1.38	6.74
20	LHAF	0.3	1.0	4	9.13	1.1	11.1
21	LHAF	0.3	1.0	4	9.02	1.4	7.35
22	LHAF	0.3	1.0	5	9.05	1.34	7.8
23	ADAF	0.1	0.89	0.8($\approx \dot{m}_1$)	9.4	0.52	0.9
24	LHAF	0.1	0.89	2	9.1	1.03	6.3
25	LHAF	0.1	0.89	2	9.4	0.52	1.6
26	LHAF	0.1	0.89	4	9.16	0.92	8.2
27	LHAF ^b	0.1	0.89	3	9.03	1.23	4.6
28	LHAF ^b	0.1	0.89	4	9.07	1.13	2.7
29	LHAF	0.01	0.5	0.1	9.6	0.19	0.05
30	LHAF	0.01	1.0	0.1	9.6	0.37	0.19

^a Models with the same α , y , and \dot{m} have different outer boundary condition.

^b There is a cold annulus transition within a certain radius in these LHAF models. In these cases, L is given for the emission of the hot flow only.

parameter is independent of the radius. While this is a simplification, we do not expect it to substantially affect our results. This is because in the case of a variable y , we can simply set the observational value of y (e.g., ≈ 0.89) at the radius where most of radiation comes from. Then, since $\dot{m} \propto rv_r\tau$, the only way that a variable y could affect our results is through modifying the radial velocity, v_r , which is not significant. The main physical reason why LHAF solutions yield lower T_e compared to the ADAF is because the former corresponds to higher accretion rates and thus higher τ .

4.1.2 The standard electron energy equation

As discussed in Section 1, global solutions including emission of soft seed photons by all possible sources is both difficult and underdetermined given our present understanding of the flow dynamics. Therefore, we have parametrized the energy equation in Section 4.1.1 by the observational constraint given by the X-ray slope. On the other hand, it is also important to check how much the presence of the additional soft photons affects our solutions. Thus, here we calculate T_e

and τ of the ADAF/LHAF solutions with a standard energy equation in which no external soft photons are included in the Comptonization process.

The results are shown in Table 3. Again we find that the obtained values of T_e in the ADAF case are too high, and thus can be ruled out for luminous sources. We also find that the LHAF without a cold annulus provides marginally appropriate values of T_e and τ in some cases, and not appropriate in some other cases (e.g., model 9 in Table 3). This indicates the importance of the Comptonization of external soft photons. On the other hand, LHAFs with a transition to a cold annulus always give appropriate values of T_e and τ . In addition, from the calculated T_e and τ of both ADAF and LHAF, we calculated y and find that it is generally $\lesssim 1$. Note that we do not include here the effect of cooling by the cold annulus.

We also present our results in Fig. 1. Comparing with the contour which corresponds to the average Seyfert-1 spectrum (ZPJ), we find that the LHAF is much more favoured than the ADAF as the accretion disc model describing the X-ray emission of Seyferts.

Table 3. Model parameters of some standard hot disc solutions.

Model	Model type ^a	α	\dot{m}	$\log(T_e \text{ [K]})$	τ	y^b	$L/L_E \text{ [%]}$
1	ADAF	0.3	$1(\approx \dot{m}_1)$	9.44	0.38	0.71	0.9
2	ADAF	0.3	1	9.46	0.34	0.66	0.7
3	ADAF	0.3	1	9.29	0.7	0.92	3.2
4	ADAF	0.3	1	9.26	0.73	0.90	3.9
5	LHAF	0.3	2	9.22	0.81	0.91	5.9
6	LHAF	0.3	3	9.24	0.76	0.89	6.0
7	ADAF	0.1	$0.1(< \dot{m}_1)$	9.85	0.05	0.24	0.004
8	ADAF	0.1	$0.5(\approx \dot{m}_1)$	9.5	0.3	0.64	0.36
9	LHAF	0.1	1	9.5	0.2	0.43	0.2
10	LHAF ^c	0.1	3	8.9	1.35	0.72	4.4
11	LHAF ^c	0.1	5	9.08	1.12	0.91	2.4
12	LHAF ^c	0.1	10	8.9	0.83	0.45	1.3

^a Models with the same α , and \dot{m} have different outer boundary condition.

^b Calculated from the T_e and τ (i.e., not a free parameter).

^c There is a cold annulus transition within a certain radius in these LHAF models. In these cases, L is given for the emission of the hot flow only.

4.2 The hard state of X-ray binaries

In Section 4.1, we have applied our model to AGNs. Here, we extend our calculations to the case of stellar-mass black holes, assuming $M = 10M_\odot$. We find that the results of our models are virtually independent of the mass. On the other hand, the data for black-hole binaries are usually much better than those for Seyferts. For example, the values of T_e are determined rather accurately for some hard states of Cyg X-1 and GX 339–4, with $T_e \approx 50\text{--}60$ keV (Frontera et al. 2001; Zdziarski et al. 1998; Wardziński et al. 2002). Such low values of T_e can hardly be reached in the ADAF case, while they are within the range of T_e predicted by the LHAF model (Table 2). (A specific application of the LHAF model to an X-ray binary, XTE J1118+480, has recently been given by Yuan, Cui & Narayan 2004.)

In addition to the value of T_e , another very strong argument in favour of the LHAF is the very large bolometric luminosity of transient (with a low-mass companion) black-hole binaries in the hard state. During the rising phase of an outburst, luminosities as high as $\sim 0.2L_E$ are observed (e.g., in XTE J1550–564, Done & Gierliński 2003; GX 339–4, Zdziarski et al. 2004, see also Nowak 1995; Maccarone 2003). Such luminosities cannot be achieved in the ADAF model, but they can (within a factor of two) be obtained by the LHAF model (see Table 2).

Narayan (1996) proposed that the variety of spectral states of black-hole X-ray binaries can be understood as a sequence of thin disc plus ADAF models with varying \dot{m} and the transition radius. This idea was developed by Esin, McClintock & Narayan (1997) and Esin et al. (1998). In their work, the hard state is associated with ADAFs with $\dot{m} \lesssim \dot{m}_1$. The advection factor f , which is a function of radius, is instead set to a value averaged over the whole accretion flow. Then f is found to have a low but still positive value, $f \sim 0.3$, at $\dot{m} \simeq \dot{m}_1$. The model typically predicts $T_e \gtrsim 10^9$ K for accretion flows within $\sim 100R_s$, and $T_e \gtrsim 10^{9.1}$ K for $r \lesssim 10R_s$ where most of the radiation comes from (see Fig. 3b in Esin et al. 1997). This is in good agree-

ment with our results, in which we also find that an ADAF predicts $T_e \gtrsim 10^{9.1}$ K. While such an ADAF model can explain the spectra of the hard state of some X-ray binaries very well, it is challenging to fit other spectra with lower energy cutoff such as Cyg X-1 and GX 339–4 because a lower $T_e \lesssim 10^9$ K is required there.

5 DISCUSSION

A caveat for our results concerns the use of the one-zone approximation of Comptonization in comparisons with prediction for T_e and τ of accretion flow models. We use it because most of the available Comptonization fits to data in astrophysical literature use the one-zone approach (i.e., a uniform electron temperature in a simple geometry). Thus, in order to compare our results with the data, we neglect the radial dependences of the temperature and density and assume that most of the radiation comes from a single radius. We intend to extend our calculation in the future by including the profiles of the electron temperature and density in the accretion flow and the non-local nature of Comptonization. On the other hand, the above approximation is not used in comparisons of the predicted and observed luminosities of black-hole binaries.

In our calculations, we assume that the accretion rate is independent of radius. Over the past few years, hydrodynamic and magnetohydrodynamic simulations (e.g., Stone, Pringle & Begelman 1999; Hawley & Balbus 2002; Igumenshchev et al. 2003) and analytical work (Narayan & Yi 1994; Blandford & Begelman 1999; Narayan et al. 2000; Quataert & Gruzinov 2000) indicate that only a fraction of the gas that is available at large radius in the accretion flow may actually accrete onto the black hole. The rest of the gas is either ejected from the flow or is prevented from accreting by convective motions. The former is due to the positive sign of the Bernoulli parameter of the accretion flow while the latter is due to the accretion flow being convection-unstable. However, all the above results are for very low

accretion rates. When the accretion rate is high, $\dot{m} \gtrsim \dot{m}_1$, as in our case, the Bernoulli parameter is negative in general, and the flow is likely to be convection-stable since the entropy of an LHAF decreases rather than increases towards the smaller radii (Paper I). Therefore, the constant accretion rate is likely a correct assumption in our case.

We also assume that the viscous dissipation mainly heats ions. Depending on some unknown details of microphysics, it is possible that a large fraction of the viscous dissipation also heats electrons (Quataert & Gruzinov 1999). If this is the case, one effect would be that the value of T_e predicted in both ADAF and LHAF will be somewhat larger for a fixed \dot{m} . This will make the ADAF even worse for describing the X-ray emission of Seyfert-1 galaxies and the hard state of X-ray binaries. Another effect of electron heating would be that the value of the critical accretion rate of ADAF, \dot{m}_1 , becomes smaller due to the weaker viscous dissipation heating of ions. In this case, the lowest T_e an ADAF can produce will become higher, which again makes the ADAF worse as the model of Seyfert-1 galaxies and X-ray binaries in the hard state and implies the occurrence of LHAFs.

There are two possible origins for the hot accretion flows. One is through the transition from an outer standard thin disc. Several mechanisms have been suggested for the transition from the outer cold disc to the inner hot disc. One is the evaporation of the cold disc due to thermal conduction (Meyer & Meyer-Hofmeister 1994; Meyer, Liu, & Meyer-Hofmeister 2000; Róžańska & Czerny 2000). The second is turbulent diffusive heat transport (Honma 1996; Manmoto et al. 2000; Manmoto & Kato 2000). The third one is the secular instability present in the radiation pressure-dominated inner region of the standard thin disc (Lightman & Eardley 1974; Gammie 1998). If the accretion flow is one-phase, then the accretion mode within R_{out} is simply determined by the accretion rate, \dot{m} . If $\dot{m} < \dot{m}_1$, it is an ADAF, otherwise it is an LHAF. If the transition is due to secular instability, the instability may result in the formation of cold clumps embedded in the hot flow. In this case, the accretion rate and accretion mode in the hot phase may depend on the interchange of matter and energy between the cold and hot phases. The emission from the cold clumps will supply additional soft photons as the seeds for Comptonization.

The second possible origin for hot accretion flow is that the accretion flow is already hot at large radii (e.g., Shlosman, Begelman & Frank 1990). First, there exists such a hot branch of accretion solution even for the accretion rates as high as Eddington (Paper I). Second, in the case of AGNs, there is strong observational evidence that hot cooling flows carry large amount of hot gas into the central region of AGNs (Sarazin 1986; Arnaud 1988) which could serve as the accretion material. The hot ISM is also a source of accreting material. In the case of X-ray binaries, if the accretion comes from the supersonic stellar wind from the companion star, the accretion flow may start out hot due to the heating of a bow shock.

6 CONCLUSIONS

In this paper, we have investigated the hot accretion disc model applied to the X-ray emission of Seyfert galaxies and black-hole binaries in the hard state. Especially, we con-

sider the luminous hot accretion flow recently found (Paper I)—LHAF—and compare it with the ADAF. We numerically solve the radiation hydrodynamical accretion equation to obtain the electron temperature and the Thomson optical depth of these two models at the radius where most of the emission comes from. We adopt two forms of the electron energy equation, with one being the standard in the sense that only synchrotron, bremsstrahlung and their Comptonization are included as the emission mechanisms, with the other parameterized by the Compton parameter, y , to approximate the actual cooling process of electrons, e.g., external soft seed photon and feedback process between cold and hot components.

Comparing our results to those obtained by fitting the observed average spectra of Seyfert-1 galaxies and black-hole binaries by thermal Comptonization models, we find: (i) the ADAF with the standard electron energy equation is ruled out due to its T_e being too high; (ii) the ADAF with external soft photon as seed photon of Comptonization is also not likely to be responsible for the X-rays; (iii) the LHAF with standard electron energy equation is marginally feasible in the sense that T_e is in the edge of the observed parameter space; (iv) the most possible accretion disc model for the X-ray emission of Seyfert-1 galaxies is an LHAF with the electron energy equation including additional sources of seed photons (parametrized by y); (v) the high bolometric luminosity of some black hole X-ray binaries in the hard states can be achieved in an LHAF but not an ADAF.

ACKNOWLEDGEMENTS

We thank R. Narayan and A. Beloborodov for helpful suggestions and discussions and J. Poutanen for valuable comments. FY was supported in part by grants from NASA (NAG5-9998, NAG5-10780) and NSF (AST 9820686), and AAZ, by the KBN grant PBZ-KBN-054/P03/2001.

REFERENCES

- Abramowicz M. A., Chen X., Kato S., Lasota J.-P., Regev O., 1995, *ApJ*, 438, L37
- Abramowicz M.A., Czerny B., Lasota J.P., Szuszkiewicz E., 1988, *ApJ*, 332, 646
- Arnaud K. A., 1988, in Fabian A. C., ed., *Cooling Flows in Clusters of Galaxies*, Kluwer, Dordrecht, p. 31
- Beloborodov A. M., 1999a, *ApJ*, 510, L123
- Beloborodov A. M., 1999b, in Poutanen J., Svensson R., eds., *ASP Conf. Ser. Vol. 161, High Energy Processes in Accreting Black Holes*. ASP, San Francisco, p. 295
- Blandford R. D., Begelman M. C., 1999, *MNRAS*, 303, L1
- Celotti A., Fabian A. C., Rees, M. J., 1992, *MNRAS*, 255, 419
- Dermer C. D., Liang E. P., Canfield E., 1991, *ApJ*, 369, 410
- Done C., Gierliński M., 2003, *MNRAS*, 342, 1041
- Deufel B., Spruit H. C., 2000, *A&A*, 362, 1
- Esin A. A., Narayan R., Ostriker E., Yi I., 1996, *ApJ*, 465, 312
- Esin A. A., McClintock J. E., Narayan R., 1997, *ApJ*, 489, 865
- Esin A. A., Narayan R., Cui W., Grove J. E., Zhang S., 1998, *ApJ*, 505, 854
- Fiore F., Perola G. C., Matsuoka M., Yamauchi M., Piro L., 1992, *A&A*, 262, 37
- Frontera F., et al., 2001, *ApJ*, 546, 1027
- Galeev A. A., Rosner R., Vaiana G. S., 1979, *ApJ*, 229, 318

- Gammie C. F., 1998, MNRAS, 297, 929
- Ghisellini G., Haardt F., 1994, ApJ, 429, L53
- Gierliński M., Zdziarski A. A., Done C., Johnson W. N., Ebisawa K., Ueda Y., Haardt F., Philips B. F., 1997, MNRAS, 288, 958
- Gondek D., Zdziarski A. A., Johnson W. N., George I. M., McNaron-Brown K., Magdziarz P., Smith D., Gruber D. E., 1996, MNRAS, 282, 646
- Guilbert P. W., Rees M. J., 1988, MNRAS, 233, 475
- Haardt F., Maraschi L., 1993, ApJ, 413, 507
- Hawley J. F., Balbus S. A., 2002, ApJ, 573, 738
- Hawley J. F., Gammie C. F., Balbus S. A., 1996, ApJ, 463, 656
- Honma F., 1996, PASJ, 48, 77
- Ichimaru S., 1977, ApJ, 214, 840
- Igumenshchev I. V., Narayan R., Abramowicz M. A., 2003, ApJ, 592, 1042
- Johnson W. N., McNaron-Brown K., Kurfess J. D., Zdziarski A. A., Magdziarz P., Gehrels N., 1997, ApJ, 482, 173
- Kato S., Fukue J., Mineshige S., 1998, Black-hole Accretion Disks, Kyoto Univ. Press, Kyoto
- Krolik J. H., 1998, ApJ, 498, L13
- Kuncic Z., Celotti A., Rees M. J., 1997, MNRAS, 284, 717
- Lightman A. P., Eardley D. M., 1974, ApJ, 187, L1
- Maccarone T. J., 2003, A&A, 409, 697
- Manmoto T., Kato S., 2000, ApJ, 538, 295
- Manmoto T., Kato S., Nakamura K. E., Narayan R., 2000, ApJ, 529, 127
- McConnell M. L., et al., 2002, ApJ, 572, 984
- Meyer F., Meyer-Hofmeister E., 1994, A&A, 288, 175
- Meyer F., Liu B. F., Meyer-Hofmeister E., 2000, A&A, 354, L67
- Nakamura K. E., Kusunose M., Matsumoto R., Kato S., 1997, PASJ, 49, 503
- Nandra K., Pounds K. A., 1994, MNRAS, 268, 405
- Nandra K., George I. M., Mushotzky R. F., Turner T. J., Yaqoob T., 1997, ApJ, 477, 602
- Narayan R., 1996, ApJ, 462, 136
- Narayan R., Yi I., 1994, ApJ, 428, L13
- Narayan R., Yi I., 1995, ApJ, 444, 231
- Narayan R., Mahadevan R., Quataert E., 1998, in Abramowicz M. A., Björnsson G., Pringle J. E., eds., The Theory of Black Hole Accretion Discs, Cambridge Univ. Press, Cambridge, p. 148
- Narayan R., Igumenshchev I. V., Abramowicz M. A., 2000, ApJ, 539, 798
- Nowak M. A., 1995, PASP, 107, 1207
- Paczynski B., Wiita P. J. 1980, A&A, 88, 23
- Poutanen, J. 1998, in Abramowicz M. A., Björnsson M. A., Pringle J. E., eds., Theory of Black Hole Accretion Discs. Cambridge Univ. Press, Cambridge, p. 100
- Poutanen J., Svensson R., 1996, ApJ, 470, 249
- Poutanen J., Krolik J. H., Ryde F., 1997, MNRAS, 292, L21
- Pringle J. E., 1976, MNRAS, 177, 65
- Quataert E., Gruzinov A., 1999, ApJ, 520, 248
- Quataert E., Gruzinov A., 2000, ApJ, 539, 809
- Rees M. J., Begelman M. C., Blandford R. D., Phinney E. S., 1982, Nature, 295, 17
- Różańska A., Czerny B., 2000, A&A, 360, 1170
- Sarazin C. L., 1986, RMP, 58, 1
- Shapiro S. L., Lightman A. P., Eardley D. M., 1976, ApJ, 204, 187 (SLE)
- Shlosman I., Begelman M. C., Frank J., 1990, Nature, 345, 679
- Spruit H. C., Haardt F., 2000, MNRAS, 313, 751
- Stone J. M., Pringle J. E., Begelman M. C., 1999, MNRAS, 310, 1002
- Wardziński G., Zdziarski, A. A., 2000, MNRAS, 314, 183
- Wardziński G., Zdziarski A. A., Gierliński M., Grove J. E., Jahoda K., Johnson W. N., 2002, MNRAS, 337, 829
- Yuan F., 1999, ApJ, 521, L55
- Yuan F., 2001, MNRAS, 324, 119 (Paper I)
- Yuan F., 2003, ApJ, 594, L99
- Yuan F., Peng Q. H., Lu J. F., Wang J. M., 2000, ApJ, 537, 236
- Yuan F., Cui W., Narayan R., 2004, ApJ, submitted (astro-ph/0407612)
- Zdziarski A. A., 1998, MNRAS, 296, L51
- Zdziarski A. A., Gierliński M., 2004, Progr. Theor. Phys., in press
- Zdziarski A. A., Johnson W. N., Done C., Smith D., McNaron-Brown K., 1995, ApJ, 438, L63
- Zdziarski A. A., Poutanen J., Mikołajewska J., Gierliński M., Ebisawa K., Johnson W. N., 1998, MNRAS, 301, 435
- Zdziarski, A. A., Lubiński, P., Smith, D. A. 1999, MNRAS, 303, L11
- Zdziarski A. A., Poutanen J., Johnson W. N., 2000, ApJ, 542, 703 (ZPJ)
- Zdziarski A. A., Leighly K. M., Matsuoka M., Cappi M, Mihara T., 2002, ApJ, 573, 505
- Zdziarski A. A., Lubiński P., Gilfanov M., Revnivtsev M., 2003, MNRAS, 342, 355
- Zdziarski A. A., Gierliński M., Mikołajewska J., Wardziński G., Smith D. M., Harmon A., Kitamoto S., 2004, MNRAS, 351, 791
- Życki P. T., Done C., Smith D. A., 1998, ApJ, 496, L25